Available online at www.sciencedirect.com
ScienceDirect
Journal of Nuclear Materials 373 (2008) 237–245
journal of nuclear materials
www.elsevier.com/locate/jnucmat

Solidus and liquidus temperatures in the UO_2–PuO_2 system

M. Kato [a,*], K. Morimoto [a], H. Sugata [b], K. Konashi [c], M. Kashimura [a], T. Abe [a]

[a] *Nuclear Fuel Cycle Engineering Laboratories, Japan Atomic Energy Agency, 4-33, Tokai-mura, Naka-gun, Ibaraki 319-1194, Japan*
[b] *Inspection Development Company, 4-33, Tokai-mura, Naka-gun, Ibaraki 319-1194, Japan*
[c] *Tohoku University, 2145-2, Narita, Oarai-machi, Ibaraki 311-1313, Japan*

Received 21 December 2006; accepted 6 June 2007

Abstract

The melting of plutonium and uranium mixed oxide containing Pu of more than 30% was investigated using a tungsten capsule and a rhenium inner capsule. In the conventional measurements of $(Pu,U)O_{2.00}$ in the tungsten capsule, a liquid phase of tungsten and plutonium oxide appeared in the mixed oxide during melting. This liquid phase was found to have an effect on the measurement of melting point. Therefore, the rhenium inner capsule was used to avoid the effect. The solidus and liquidus temperatures in the UO_2–PuO_2 system were decided from the $(Pu,U)O_{2.00}$ data measured using the rhenium capsule, and the effect of the Am content on the solidus temperature was evaluated. The variation of the solidus and liquidus temperatures in the UO_2–PuO_2–AmO_2 ternary system was represented to an accuracy of $\sigma = \pm 9$ K and $\sigma = \pm 16$ K, respectively, by the ideal solution model.

PACS: 64.70.Dv; 81.30.Bx

1. Introduction

Plutonium and uranium mixed oxide (MOX) containing 30%Pu has been developed as the core fuel pellet of the fast reactor *Monju* [1]. The fuel pellet temperature rises to over 2300 K during irradiation because of the high linear heating power. The large temperature gradient in the radial direction causes redistribution of Pu and U, and Pu content increases to about 40% at the pellet center [2,3]. The maximum temperature of the fuel pellet during irradiation is limited within the design criterion to prevent fuel melting. So, it is essential to know the melting point of MOX as a function of Pu content.

Plutonium material used in the fuel contains a small amount of americium which is a daughter nuclide of ^{241}Pu. Americium content in the fuel for the fast reactor will be increased and this must be taken into account for long-term storage. Therefore, it is also necessary to investigate the effect of Am content on the melting point of MOX.

Lyon and Baily [4] and Aitken and Evans [5] measured the melting points of MOX systematically using the thermal arrest technique. In both reports, however, after the experiment, the samples were not analyzed for any change which might have occurred during heating. Most recently the authors [6] also measured the melting point of MOX as a function of Pu content, and reported that the measured solidus temperatures were in good agreement with the data of Lyon and Baily [4]. The authors also showed the solidus temperature decreased with increasing PuO_2 content and suddenly dropped at the composition between 20% and 30%Pu [6]. The melted samples were analyzed and were observed to contain a large amount of metallic W and Pu oxide along the grain boundary of the samples with 30% and 40%Pu content. It was suggested that the discontinuous variation of the solidus was caused by reaction with W that came from the capsule which the sample was sealed inside.

To investigate the effect of the reaction between W and the specimen on the measured melting point, it is necessary to carry out experiments eliminating the effect of the capsule material. In this work, a Re inner capsule was

* Corresponding author. Tel.: +81 29 282 1111; fax: +81 29 282 9473.
E-mail address: kato.masato@jaea.go.jp (M. Kato).

0022-3115/$ - see front matter © 2007 Elsevier B.V. All rights reserved.
doi:10.1016/j.jnucmat.2007.06.002

employed to prevent the reaction and the melting points were measured. The dependence of changes of the microstructure on heating temperature was investigated for both W and Re capsules, and the melting temperatures were decided for the UO_2–PuO_2 system. In addition, the effect of the Am content on solidus temperature was evaluated.

2. Experimental

2.1. Sample preparation

The sintered pellets listed in Table 1 were prepared by a mechanical blending method, and powders of UO_2, $(U_{0.513}Pu_{0.463}Am_{0.024})O_2$, $(Pu_{0.979}Am_{0.021})O_2$ and $(Pu_{0.926}Am_{0.074})O_2$ were used as raw materials. Americium included in the powders was accumulated during the long-term storage due to β-decay of ^{241}Pu. The mixed powder was pressed and sintered at 1973 K for 3 h in an atmosphere of Ar and 5%H_2 gas mixture with added moisture. The oxygen-to-metal (O/M) ratio of the sintered pellets was adjusted to 2.00 by annealing at 1023 K for 5 h at the oxygen potential of $\Delta\overline{G}_{O_2} \cong -400$ kJ/mol. The sum of metallic impurities in the pellet was less than 500 ppm. All of the samples were analyzed with an X-ray diffractometer (XRD: Rigaku RINT-1100) and an electron probe micro analyzer (EPMA: JEOL JXA8800), and were confirmed to be homogeneous.

2.2. Measurement procedure

Five types of capsules (Fig. 1) were prepared. Types C, D and E had a Re inner capsule. The W capsules were sealed in vacuum by electron beam welding. Two kinds of experiments were carried out to measure the melting point and to observe the dependence of the change of the microstructure on heating temperature; the conditions are listed in Tables 1 and 2, respectively.

In the measurement of the melting point the samples shown in Fig. 1 were heated above the melting points at a constant heating rate of 40–80 K/min, and heating temperature curves were obtained. The apparatus and procedures used in this experiment were similar to those described previously [4–10] for determining the melting point of MOX.

Temperatures were measured with a pyrometer placed in the black body well at the bottom end cap of the W capsule

Table 1
Samples and measured melting temperature

No.	Composition				Type of cell	Temperature of arrest		W content (%) after heating
	U (%)	Pu (%)	Am (%)	O/M		Starting point (K)	Ending point (K)	
1	69.6	29.8	0.6	2.000	C	3030	3074	–
2	59.6	39.7	0.7	2.000	C	2997	3029	–
3	59.6	39.7	0.7	2.000	C	3009	3020	–
4	58.5	39.6	1.9	2.000	C	3000	3052	–
5	58.5	39.6	1.9	2.000	C	3006	3043	–
6	58.4	38.3	3.3	2.000	C	2988	3017	–
7	58.4	38.3	3.3	2.000	C	2998	3050	–
8	58.4	38.3	3.3	2.000	C	3010	3039	–
9	51.4	46.3	2.4	2.000	C	2971	2998	–
10	37.7	60.0	2.3	2.000	C	2940	–[b]	
11	–	97.9	2.1	2.000	C	2822	2938	–
12	100	0	0	2.000	A	3140[a]	–	0
13	88.0	11.7	0.3	2.000	A	3077[a]	3117[a]	0
14	88.0	11.7	0.3	1.989	A	3093[a]	3135[a]	0
15	88.0	11.7	0.3	1.983	A	3084[a]	3105[a]	0
16	88.0	11.7	0.3	1.975	A	3085[a]	3107[a]	0
17	88.0	11.7	0.3	1.974	A	3054[a]	3069[a]	0
18	88.0	11.7	0.3	1.971	A	3100[a]	3124[a]	0
19	79.8	19.8	0.4	2.000	A	3052[a]	3090[a]	<1
20	79.8	19.8	0.4	1.982	A	3059[a]	3089[a]	<1
21	79.8	19.8	0.4	1.967	A	3066[a]	3079[a]	<1
22	79.8	19.8	0.4	1.954	A	3074[a]	3109[a]	<1
23	79.8	19.8	0.4	1.950	A	3079[a]	3097[a]	<1
24	79.8	19.8	0.4	1.942	A	3092[a]	3118[a]	<1
25	70.0	29.7	0.3	2.000	A	2967[a]	3047[a]	14
26	70.0	29.7	0.3	1.983	A	2979[a]	3073[a]	8
27	70.0	29.7	0.3	1.966	A	3025[a]	3062[a]	7
28	70.0	29.7	0.3	1.939	A	2995	3038	10
29	70.0	29.7	0.3	1.922	A	3041	3055	4
30	59.7	39.8	0.5	2.000	A	2910[a]	3024[a]	19–20
31	59.0	40.0	1.0	1.885	A	2981	3018	11.2

[a] Melting points were reported in previous works [6,10].
[b] The arrest was not detected during heating up to 2992 K.

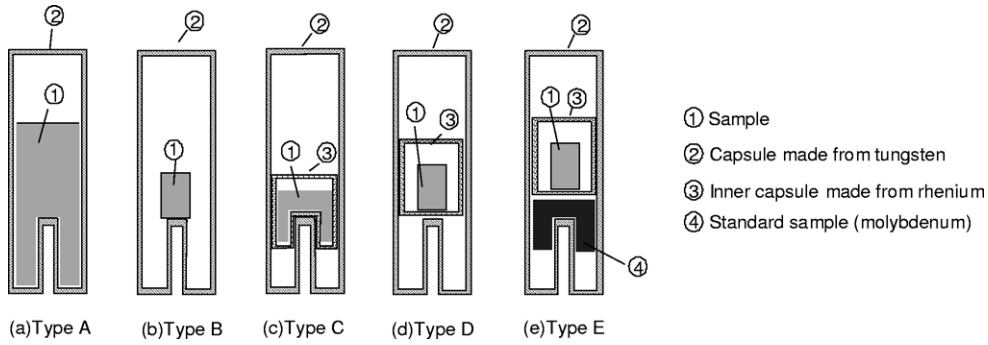

Fig. 1. Schematic diagram of cell: (a) W capsule with crushed pellet, (b) W capsule with a pellet, (c) a Re inner capsule with sintered sample which was sealed in a W capsule, (d) a Re inner capsule with a pellet which was sealed in a W capsule and (e) a standard sample and a Re inner capsule with pellet which were sealed in a W capsule.

Table 2
Test condition and results in observation of microstructures of $(Pu_{0.397}Am_{0.007}U_{0.596})O_{2.00}$

Sample no.	Type of cell	Shape of sample	Test condition	Appearance after heating
W-1	B	Pellet	2868 K × 5 min	[a]
W-2	B	Pellet	2963 K × 5 min	[b]
W-3	B	Pellet	3023 K × 5 min	[b]
W-4[c]	A	Crushed pellet	Heating up to 3090 K, 80 K/min	[b]
Re-1	E	Pellet	2895 K × 1 min	[a]
Re-2	D	Pellet	2903–2927 K × 2 min	[a]
Re-3	C	Crushed pellet	Heating up to 3031 K	[b]
Re–4	C	Crushed pellet	Heating up to 3070 K, 40 K/min	[b]
Re-5	C	2nd test of Re-4	Heating up to 3090 K, 40 K/min	[b]

[a] Original shape of pellet.
[b] Deformed block.
[c] Melting point was reported in previous works [6].

as shown in previous work [10]. The temperature was calibrated by measuring the melting points of tantalum, molybdenum, niobium and alumina, which were reported to be 3280, 2895, 2745, and 2326 K, respectively [11]. The measurement of the standard samples for calibration was done using a capsule type C with W inner capsule instead of Re. The calibration curve was made to obtain the true temperature from the observed temperature. The uncertainty limit of the melting points was estimated to be ±35 K from the uncertainty in measuring the melting points of the standard samples and in determining the melting point from the heating curve.

Samples to observe microstructure were heated under the conditions shown in Table 2 and then cooled below 1000 K at the cooling rate of greater than 100 K/min. After heating, the samples were removed from the capsules and were analyzed by ceramography, XRD and EPMA. The results were compared with the data measured before heating.

3. Results and discussion

3.1. Effect of reaction with capsule materials on the measurement of melting point

Typical heating temperature curves are shown in Fig. 2. The arrests were observed clearly in both heating curves as shown by arrows. The starting and ending points of the arrest were considered to correspond to solidus and liquidus temperatures, respectively. The microstructures and appearances of samples after heating are shown in Fig. 3 and Table 2, respectively. The sample W-1 was heated to a temperature below the starting point of the arrest, and the shape of the original pellet was kept after the heating treatment. The sample W-2 was heated to a higher temperature than W-1. According to its heating curve, the maximum temperature of W-2 exceeded the solidus temperature. This was confirmed by visual inspection of the sample after heating (Table 2). The results of metallographic examination in Fig. 3(b) show grain growth and aggregation of pores occurred due to heating to high temperature. Samples W-3 and W-4 had finer grains and pores

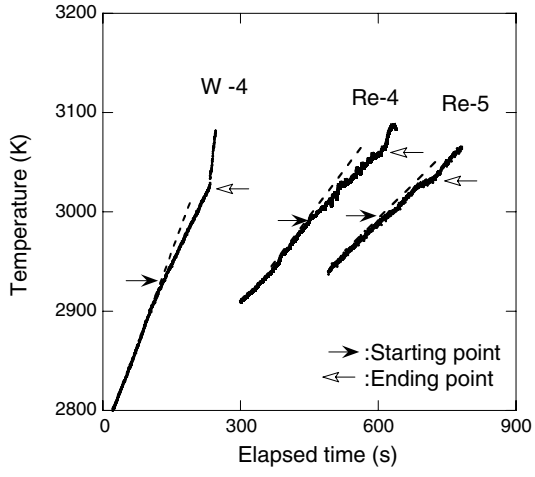

Fig. 2. Comparison of heating curves of $(Pu_{0.397}Am_{0.007}U_{0.596})O_{2.00}$ heated by using W-4, Re-4 and Re-5 capsules.

compared with W-1 and W-2. This indicates that liquid phase spreads in the sample at the heating temperature. In fact W-3 and W-4 were heated to almost the liquidus temperature and to the temperature exceeding the liquidus temperature of the arrest, respectively. The fine grains and pores were created during the solidification process.

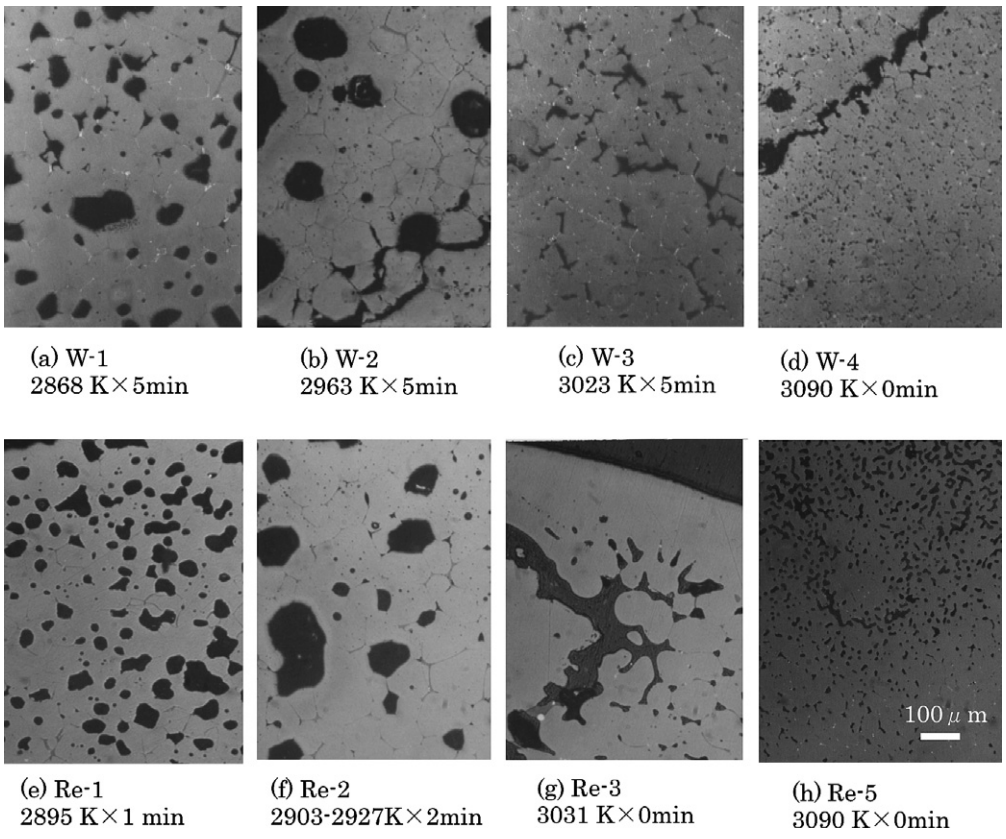

Fig. 3. Microstructures of $(Pu_{0.397}Am_{0.007}U_{0.596})O_{2.00}$ after heating.

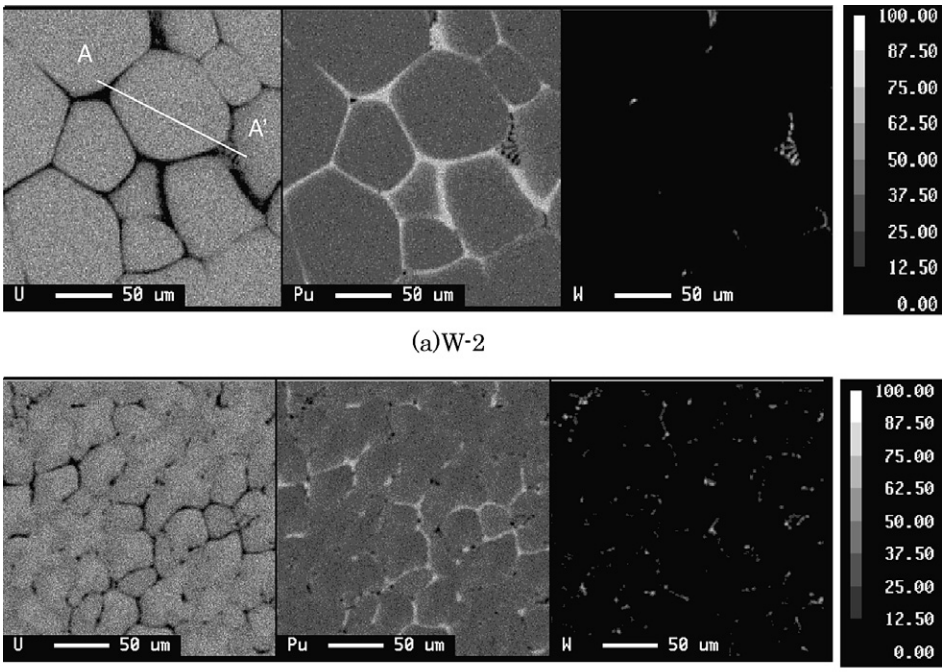

Fig. 4. Mapping images on a cross section of W-2 and W-4 samples analyzed by EPMA. **Mapping image was reported in previous works [6].

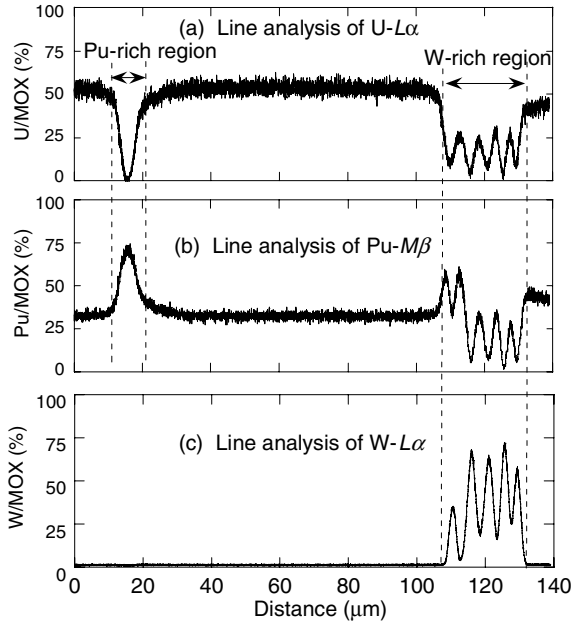

Fig. 5. Line analyses of U-L_α, Pu-M_β and W-L_α on a cross section of W-2 sample.

Figs. 4 and 5 show the mapping images and line analysis, respectively, of U-L_α, Pu-M_β and W-L_α on a cross section of W-2. The line analysis in Fig. 5 was carried out along the line of A–A′ shown in Fig. 4(a). There were Pu-rich and W-rich regions along the grain boundary. The W in the melted sample was identified as metal by XRD. The results of EPMA showed that the Pu-rich phase was a Pu oxide without U and the W-rich phase was a tangled phase of W and MOX like a eutectic phase. Fig. 6 shows the microstructures on a cross section of W-2 and W-4 samples obtained by ceramography. Fig. 6(a) shows the microstructure of W-2 sample including the W-rich phase, which appeared all over the sample. Fig. 4(b) shows mapping images of W-4 which was heated above the ending point of the arrest. The phases of Pu oxide and W were observed along the grain boundary in W-4 as well as in W-2. However, the tangled phase of W and MOX like the phase observed in W-2 was not observed clearly in W-4 as shown in Fig. 6(b) because of its fine size. These observations suggested that the arrest in the heating curves of W-4 in Fig. 2 was related to the appearance of the liquid phase of W and Pu oxide.

The analyzed results of XRD and EPMA showed that W exists in the melted sample as metal but not oxide and dissolved W. The amount of the metallic W existing in the melted sample was estimated using X-ray diffraction data. Fig. 7 shows this as a function of O/M ratio of MOX. The MOX samples with low Pu content (less than 20%) are shown by open triangles. The W content decreased drastically at the O/M of 2.0. In the region of hypostoichiometric composition (O/M < 2.0), only a small amount of W impurities (1–2%) was found in the sample after the melting experiment. These results agreed with Latta and Fryxell's experimental results with $UO_{2\pm x}$ samples [7] (open circles in Fig. 7). On the other hand, large amounts of W were found in the MOX samples with high Pu contents of 30% and 40%. This showed W existing into the Pu-rich MOX sample and may have affected the measurement of the melting point even in the region of low O/M ratio.

As described above, the results of metallographic examinations showed a large amount of W existing into MOX samples in the W-series samples. In the next experiment, Re inner capsules were applied to avoid the impurity effect on melting. Rhenium is known to be quite inert to $UO_{2\pm x}$ and MOX.

The sample Re-1 with capsule type E was heated to the melting point of Mo, which is lower than the solidus temperature. Sample Re-2 was heated to a higher temperature of 2927 K (this was higher than the solidus temperature measured with a W capsule), and grain growth was observed as shown in Fig. 3. The microstructure of Re-5 had fine crystal grains and pores, suggesting that Re-5 was cooled from the liquid phase. Microstructure was not observed for Re-4 because Re-4 was heated again as the sample Re-5. In the heating temperature curve of Re-5

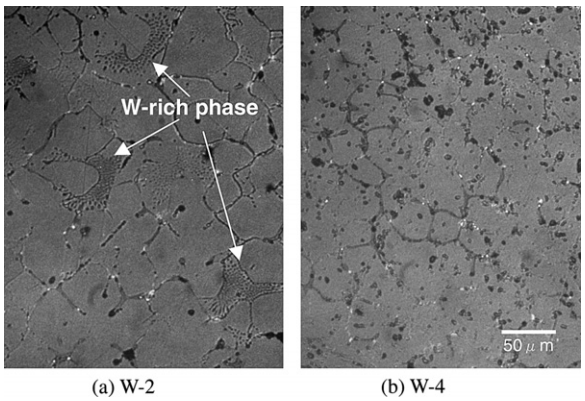

Fig. 6. Microstructure of W-2 and W-4 samples after melting temperature measurement.

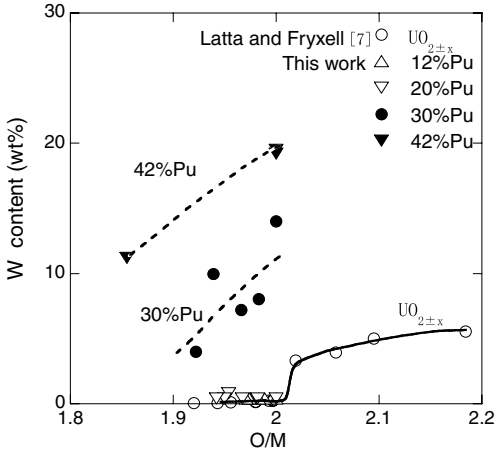

Fig. 7. Variation of W content contained in the melted samples.

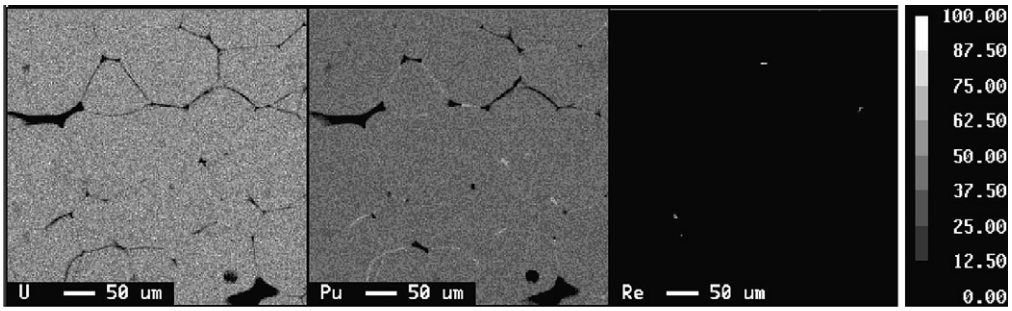

(a) Re-3

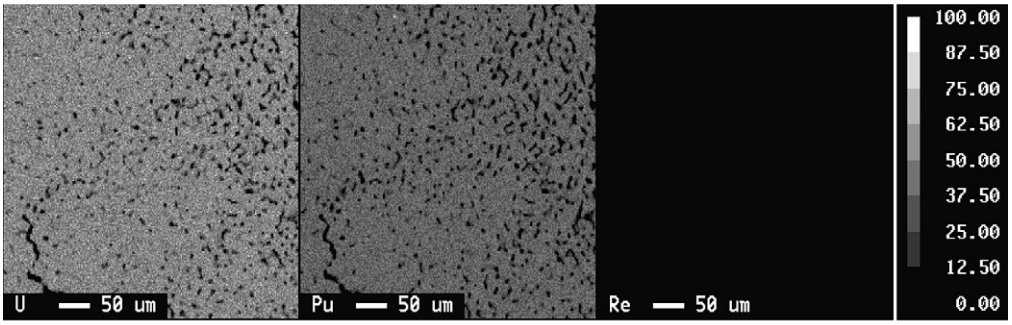

(b) Re-5

Fig. 8. Mapping images on a cross section of Re-3 and Re-5 samples analyzed by EPMA.

the arrest was also observed at almost the same temperature as that of Re-4. Such a change of microstructure in the Re-series samples was also consistent with the temperatures of the arrest shown in Fig. 2. Fig. 8 shows the mapping images of Re-3 and Re-5 samples which were cooled from a temperature above the solidus temperature. A very small quantity of Re impurity in MOX sample, less than 1%, was found. The microstructure of Re-5 showed fine crystal grains, which were formed during solidifying from liquid phase.

Fig. 9 compares experimental results of solidus temperatures for W capsules and Re capsules. The solidus temperatures with W capsule were lower than those with the Re capsule in the region of Pu content larger than 30%. It could be concluded that the solidus temperature measured by using the Re inner capsule was the true melting temperature of MOX.

3.2. The solidus and liquidus temperatures

The solidus and liquidus temperatures were measured using the capsule type C with a Re inner capsule and the heating curves of sample Nos. 1, 2 and11 are shown in Fig. 10. The starting and ending points of the arrest are shown in Table 1 and Fig. 11. Data from other works [4–6,14,16] are also plotted in Fig. 11 for comparison; these were measured using a W capsule like type A. Previously

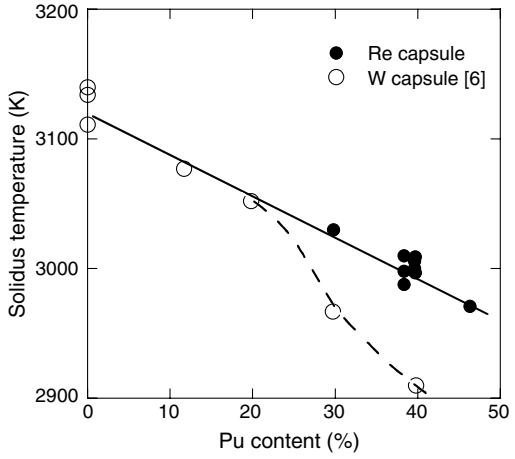

Fig. 9. Comparison of solidus temperatures obtained with Re and W capsules.

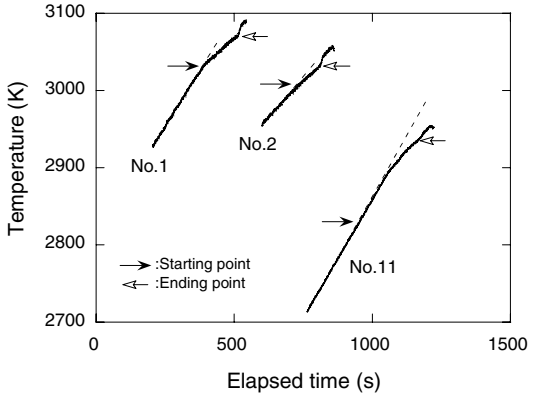

Fig. 10. Heating curves of Sample No. 1: $(U_{0.696}Pu_{0.298}Am_{0.006})O_{2.00}$, No. 2: $(U_{0.596}Pu_{0.397}Am_{0.007})O_{2.00}$ and No. 11: $(Pu_{0.979}Am_{0.021})O_{2.00}$.

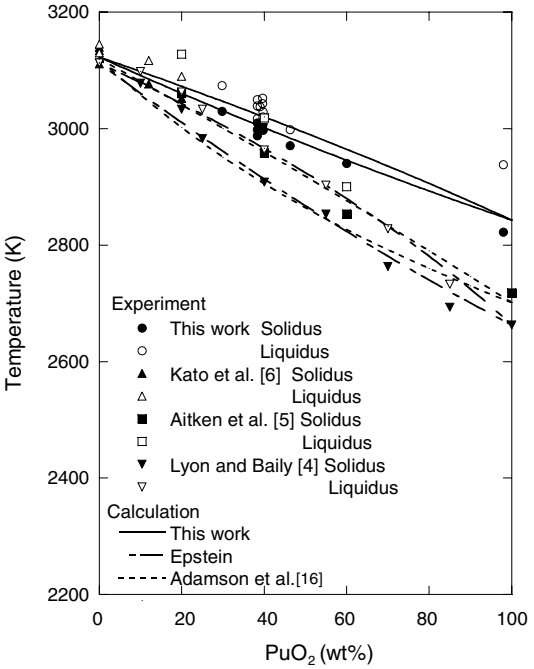

Fig. 11. Solidus and liquidus temperatures in the UO_2–PuO_2 system.

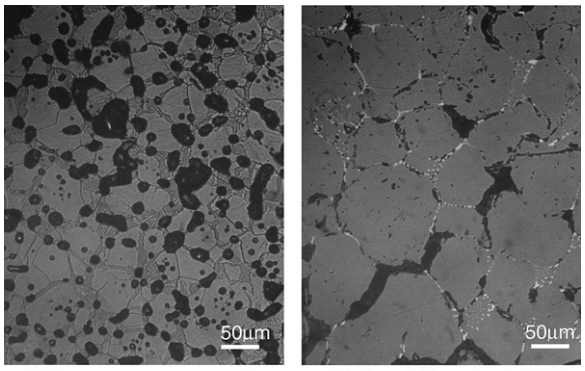

Fig. 12. Microstructure of $(Pu_{0.979}Am_{0.021})O_2$ samples after heating.

[6], it was reported that the solidus temperature measured for MOX contained W capsule decreased with an increase of Pu oxide content and it dropped significantly at a composition between 20% and 30%PuO_2. The melting point of the samples with 0–20%PuO_2 content was measured without reacting with W in the previous work [6], and the higher Pu-containing MOX was observed to react with W during melting and to decrease the solidus temperature. In Fig. 11, the present data measured using a Re capsule are also plotted, and the measured solidus temperature was consistent with the variation of solidus temperature for 0–20%PuO_2 content. The solidus temperature of $(Pu_{0.4}U_{0.6})O_{2.00}$ was about 100 K higher than the existing data that were measured using a W capsule.

The experiments of $(Pu_{0.979}Am_{0.021})O_2$ were carried out two times, and the samples heated up 2808 K and 2976 K, respectively. In the sample heated to 2808 K, the transformation in the appearance was not observed, and a trace of melting was not also found out. However, it was observed that the microstructure decomposed two phases of $PuO_2 + PuO_{1.52}$ as shown Fig. 12(a) and the O/M decreased to about 1.90. On the other hand the sample heated to 2976 K was observed to transform to a block, and the arrest was detected in the heating curve as shown in Fig. 10. The microstructure of the heated sample is shown in Fig. 12(b). It was observed that the reaction between Re and the sample occurred.

It is well-known that PuO_2 has the higher oxygen potential in the UO_2–PuO_2 system [12,13]. In the measurement of $(Pu_{0.979}Am_{0.021})O_2$, the reaction between Re and the sample and the decrease of the O/M ratio were observed even in the measurement using the Re capsule. It was considered that oxidation of Re caused the reduction of the sample due to its high oxygen potential. Such change of sample during measurement causes a large error in determining melting point. There was a large difference between the measured solidus and liquidus temperatures of $(Pu_{0.979}Am_{0.021})O_2$ as shown in Fig. 10, which would be caused by the reaction with Re. The measured melting point of $(Pu_{0.979}Am_{0.021})O_2$ should be expected to deviate from the true melting point, and the deviation would be larger than the measuring error.

Epstein [14] and Komatsu et al. [15] evaluated the solidus and the liquidus temperatures assuming that the UO_2-PuO_2 binary system is an ideal solution. Adamson et al. [16] and Carbajo et al. [17] derived a polynomial from experimental data to represent the variation of the solidus and the liquidus in the UO_2–PuO_2 system. And Konno et al. [8] modified the polynomial reported by Adamson et al. [16] to represent the effect of Am content, O/M ratio and burn-up. All of the represented melting points were consistent with the data for MOX of more than 30%Pu content that were measured with a W capsule. In the present study, the measured solidus and liquidus temperatures were analyzed assuming that UO_2–PuO_2–AmO_2 ternary system is an ideal solid solution using the data in this work and the previous work [6].

In the ternary solid solution, composition and melting temperature are obtained by simultaneously solving the following equations:

$$\frac{\Delta h_m(UO_2)}{R}\left(\frac{1}{T_m(UO_2)}-\frac{1}{T_m}\right)=\ln\left(\frac{x^l(UO_2)}{x^s(UO_2)}\right), \quad (1)$$

$$\frac{\Delta h_m(PuO_2)}{R}\left(\frac{1}{T_m(PuO_2)}-\frac{1}{T_m}\right)=\ln\left(\frac{x^l(PuO_2)}{x^s(PuO_2)}\right), \quad (2)$$

$$\frac{\Delta h_m(AmO_2)}{R}\left(\frac{1}{T_m(AmO_2)}-\frac{1}{T_m}\right)=\ln\left(\frac{x^l(AmO_2)}{x^s(AmO_2)}\right), \quad (3)$$

$$x^l(UO_2)+x^l(PuO_2)+x^l(AmO_2)=1, \quad (4)$$

$$x^s(UO_2)+x^s(PuO_2)+x^s(AmO_2)=1, \quad (5)$$

where T_m is the melting temperature of the (Pu, Am, U)$O_{2.00}$ solution, $T_m(i)$ and $\Delta h_m(i)$ are melting temper-

ature and heat of fusion at $T_m(i)$, respectively, of the pure substance i, $x^l(i)$ and $x^s(i)$ represent the mole fractions of component i in the liquid and the solid solutions, respectively, and R is the gas constant. In the case of a compound of MO_2, the relation in $T_m(i)$ and $\Delta h_m(i)$ is described by the following equation [14,18,19]:

$$\Delta h_m(i) = 3RT_m(i). \quad (6)$$

The solidus and the liquidus temperatures in (Pu, Am, U)$O_{2.00}$ are represented by deciding $T_m(i)$ using Eqs. (1)–(6). The measured data in this work were fitted as a function of $T_m(i)$, and $T_m(i)$ and $\Delta h_m(i)$ obtained are shown in Table 3. The calculated solidus and liquidus are shown in Figs. 11 and 13. The derived model represented well the experimental data as a function of PuO_2 and AmO_2 contents. The effect of Am content on the solidus temperature was slight, causing a decrease of about 4 K per 1%AmO_2.

Table 3 also shows the data from other sources for comparison. The T_m and Δh_m of UO_2 were in good agreement with the other data. In the present study, the melting point of PuO_2 was measured and evaluated to be about 200 K more than that in the other works, and the $\Delta h_m(PuO_2)$ was almost in agreement with the other data. McHenry [20] used the V-filament technique to measure melting point of AmO_2 which was reported to be 2130 K. Assuming that the melting point of AmO_2 was about 300 K higher than that measured by McHenry [20], the calculated result was consistent with the experimental data. The solidus and liquidus temperatures calculated as a function of PuO_2 and AmO_2 had a standard deviation of $\sigma = \pm 9$ K and $\sigma = \pm 16$ K, respectively, such as shown in Figs. 11 and 13. The liquidus temperature had a larger deviation than the solidus temperature. In the heating process, the liquid phase appears easily along grain boundaries at the solidus temperature. And then the progress of the melting changes the composition and volume fraction in the solid and liquid phase. However the equilibrium in melting is not reached for a short time like the measurement time. Therefore the measured liquidus has a larger deviation compared with the solidus.

Table 3
Comparison of melting points and heat of fusion of UO_2, PuO_2 and AmO_2

	Melting temperature (K)			Heat of fusion CR (kJ/mol)		
	UO_2	PuO_2	AmO_2	UO_2	PuO_2	AmO_2
This work	3123	2843	2773	77.9	70.9	69.1
Epstein [14]	3113	2662		77.8	66.5	
Epstein [14]	3113	2662		88.7	70.3	
Adamson et al. [16].	3120	2701		86.9	90.5	
Komatu et al. [15]	3138	2718		77.8	66.5	
Zhang et al. [18,19]	3140	2663	2448	78.0	67.0	61.1

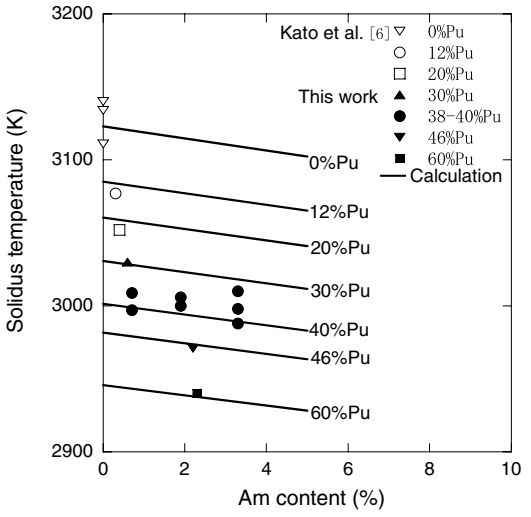

Fig. 13. The effect of Am content on solidus temperature.

4. Conclusion

The MOX pellets with 40%Pu content were heated in capsules made of W and Re, and the MOX melting behavior was investigated. The interactions of capsules with MOX samples were carefully checked. In the experiments with the W capsule, it was found that the reaction between W and MOX occurred during the heating, and Pu oxide and metallic W were precipitated along the grain boundaries in the sample cooled from two phase region of solid and liquid. It was concluded that the meting temperatures measured with W capsule were not the true value of MOX. On the other hand, the MOX heated with Re inner was confirmed to have little reaction with capsule materials during the measurement, and the measured arrests were about 100 K higher than those with W capsule.

The solidus and liquidus temperatures of MOX with 29.8–60.0%Pu were measured with Re inner and decided from the arrest observed in the heating curves. The present solidus temperatures were consistent with the authors' previous data[16] for $(Pu_x, U_{1-x})O_{2.00}$ $(x = 0–0.2)$. The $(Pu_{0.979}Am_{0.021})O_{2.00}$ was also measured with Re inner, but the melting temperature was not decided because of the reaction with Re occurred during the heating. The model on melting temperatures for the MOX with $AmO_{2.00}$ has been developed as a function of composition ($PuO_{2.00}$, $UO_{2.00}$ and $AmO_{2.00}$ fraction) based on the ideal solution model. This model reproduced well the solidus temperatures in the UO_2–PuO_2–AmO_2 system. The effects of AmO_2 on solidus temperature were estimated to be a decrease of about 4 K per 1%AmO_2.

Acknowledgement

The authors are pleased to acknowledge Mr H. Uno, Mr T. Tamura and Mr K. Shibata for their collaboration in the sample preparation, EPMA analysis, ceramography and XRD. The authors wish to thank Dr R.J.M. Konings and his co-workers at ITU, Dr Sudreau and his co-workers

at CEA, Dr J.R. Kennedy at INL and Dr K.J. McCellan at LANL for helpful discussions.

References

[1] K. Asakura, T. Yamaguchi, T. Ohtani, J. Nucl. Mater. 357 (2006) 126.
[2] M. Bober, G. Schumacher, D. Geithoff, J. Nucl. Mater. 47 (1973) 187.
[3] T. Ishii, T. Asaga, J. Nucl. Mater. 294 (2001) 13.
[4] W.L. Lyon, W.E. Baily, J. Nucl. Mater. 22 (1967) 332.
[5] E.A. Aitken, S.K. Evans, A thermodynamic data program involving plutonium and urania at high temperatures, AEC Research and Development Report GEAP-5672, 1968.
[6] M. Kato, K. Morimoto, H. Sugata, K. Konashi, M. Kashimura, T. Abe, J. Alloys Compd. in press, doi:10.1016/j.jallcom.2007.01.183.
[7] R.E. Latta, R.E. Fryxell, J. Nucl. Mater. 35 (1970) 195.
[8] K. Konno, T. Hirosawa, J. Nucl. Sci. Technol. 397 (2002) 771.
[9] K. Yamamoto, T. Hirosawa, Y. Yoshikawa, K. Morozumi, S. Nomura, J. Nucl. Mater. 204 (1993) 85.
[10] K. Morimoto, M. Kato, U. Uno, A. Hanari, T. Tamura, H. Sugata, T. Sunaoshi, S. Kono, J. Chem. Solids 66 (2005) 634.
[11] R.E. Bedford, G. Bonnier, H. Maas, F. Pavese, Metrologia 33 (1996) 133.
[12] R.E. Woodley, J. Nucl. Mater. 96 (1981) 5.
[13] T.M. Besmann, T.B. Lindemer, J. Nucl. Mater. 130 (1985) 489.
[14] L.F. Epstein, J. Nucl. Mater. 22 (1967) 340.
[15] J. Komatsu, T. Tachibana, K. Konashi, J. Nucl. Mater. 154 (1988) 38.
[16] M.G. Adamson, E.A. Aitken, R.W. Caputi, J. Nucl. Mater. 130 (1985) 349.
[17] J.J. Carbajo, G.L. Yoder, S.G. Popv, V.K. Ivanov, J. Nucl. Mater. 299 (2001) 181.
[18] H. Zhang, M.E. Huntelaar, R.J.M. Konings, E.H.P. Cordfunke, J. Nucl. Mater. 249 (1997) 223.
[19] H. Zhang, R.J.M. Konings, M.E. Huntelaar, E.H.P. Cordfunke, J. Nucl. Mater. 250 (1997) 88.
[20] R.E. McHenry, Trans. Am. Nucl. Soc. 8 (1965) 615.